

LOOSE COUPLING OF SPECTRAL AND SPATIAL MODELS FOR MULTI-CHANNEL DIARIZATION AND ENHANCEMENT OF MEETINGS IN DYNAMIC ENVIRONMENTS

Adrian Meise^{*1}, Tobias Cord-Landwehr^{*1}, Christoph Boeddeker¹, Marc Delcroix²,
Tomohiro Nakatani², Reinhold Haeb-Umbach¹

¹Paderborn University, Germany ²NTT, Inc., Japan

ABSTRACT

Sound capture by microphone arrays opens the possibility to exploit spatial, in addition to spectral, information for diarization and signal enhancement, two important tasks in meeting transcription. However, there is no one-to-one mapping of positions in space to speakers if speakers move. Here, we address this by proposing a novel joint spatial and spectral mixture model, whose two submodels are loosely coupled by modeling the relationship between speaker and position index probabilistically. Thus, spatial and spectral information can be jointly exploited, while at the same time allowing for speakers speaking from different positions. Experiments on the LibriCSS data set with simulated speaker position changes show great improvements over tightly coupled subsystems.

Index Terms— mixture models, meeting processing, diarization, source separation

1. INTRODUCTION

Automatic meeting transcription is commonly understood to comprise the tasks of diarization, answering the question of who speaks when, of speech enhancement, which includes the separation of overlapped speech, and of Automatic Speech Recognition (ASR).

Diarization, which consists of the subtasks segmentation and speaker (re-)identification, started out heavily relying on spatial information in the context of meeting scenarios [1, 2, 3]. Following that, more recent models mostly employed purely spectral approaches: Speaker embedding vectors, which capture a spectral profile of a speaker, are extracted from segments of speech and are then clustered to obtain the diarization result [4], or are directly used to perform frame-level activity classification as in End-to-End Neural Diarization (EEND) techniques [5, 6]. A combination of both approaches, as proposed in [7], can overcome the limitations of either system and is the basis of the widely used tools Pyannote and Diarizen [8, 9]. While current systems again work on incorporating multi-channel information [10, 11, 12], these systems still primarily focus on the spectral information of a single channel and use the spatial cues as auxiliary information.

If the signals are recorded by a microphone array, spatial information can also be exploited to improve the speech enhancement quality. Array processing is well-established in the speech enhancement and source separation field, where both model-based, neural, and hybrid approaches have demonstrated significant performance gains over single-channel solutions [13]. In [14], a complex Angular Central Gaussian Mixture Model (cACGMM) is employed, which models the spatial properties of the signal. Here, a mixture component corresponds to a position in space that is assumed to uniquely

identify a speaker. The aforementioned cACGMM is also the model underlying Guided Source Separation (GSS) [15]. GSS takes the speech activity information of a preceding diarization stage as prior information for Expectation-Maximization (EM)-based model parameter estimation: The prior probabilities of the mixture components are clamped to zero if the preceding diarization indicates that the associated speaker is silent. The estimated affiliation values are the sought-after speaker activity probabilities at time-frequency (tf) resolution. They are then used for source extraction, either by masking or by beamforming.

Instead of cascading diarization and enhancement, spatial information can also be leveraged in joint diarization and enhancement/separation approaches, where diarization and separation are coupled to benefit each other. This introduces additional challenges since voice characteristics need to be associated with positions that may change over the course of the recording.

An example of such an integration is Speaker Separation via Neural Diarization (SSND) [16], which uses a multi-channel EEND system to estimate short-time speaker embeddings, which are then processed jointly with the audio signal in a subsequent separation stage.

A purely model-based approach to joint diarization and enhancement has been proposed in [17], where a spectral mixture model utilizing short-time speaker embeddings has been integrated with a spatial mixture model: they share a common latent source activity variable. Estimating its posterior probability gives tf-masks that incorporate both spectral and spatial information.

However, this method for combining spectral and spatial information performs a tight integration of the spatial and spectral models, i.e., it is based on the assumption that there is a one-to-one mapping of speaker location to speaker identity. Put differently, an underlying, crucial assumption is that speakers do not move. The goal of this paper is to relax this assumption and allow that the same speaker may speak from different positions in space. To achieve this, we propose a novel spectral-spatial mixture model, which we call a loosely coupled model. In this model, the tight coupling of the original integrated model [17] is released, and a probabilistic dependency between the spatial and the spectral mixture components is introduced, which in turn allows mapping multiple spatial mixture components to a single spectral mixture component. Being model-based, the system does not require a training stage. This makes it operate on arbitrary microphone array configurations.

In the next section we first briefly describe the tightly integrated model-based spectral-spatial diarization system of [17] and show in Section 3 how it can be relaxed to a loose coupling. The key component is the conditional probability of a spatial mixture component, given the spectral one. An important aspect is how to estimate tf-masks for source extraction in this model, to which we present a

^{*}Authors contributed equally

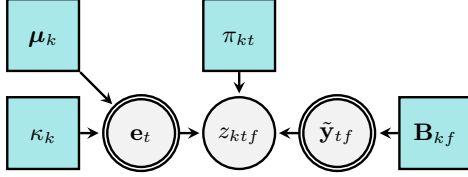


Fig. 1. Graphical model of the tight integration from [17]. The spectral model (left) and the spatial model (right) are coupled through the common latent variable z_{ktf} .

solution in Section 3.1. Experiments on the LibriCSS data set in Section 4 with simulated speaker position changes demonstrate the greatly increased insensitivity to speaker position changes compared to a tight integration of spectral and spatial diarization components.

2. MIXTURE MODEL-BASED INTEGRATION OF SEPARATION & DIARIZATION

In [17], diarization and speech separation were jointly addressed by modeling them by two statistical mixture models that are coupled through a common latent variable \mathcal{Z} representing the speech activity of each speaker per tf-bin. This mixture model aims to estimate these categorically distributed latent variables z_{ktf} given a set of observations $\mathcal{O} = \{\mathcal{O}_t \ \forall t\}$. Given a meeting recording with C microphones, these observations are $\mathcal{O}_t = \{\{\tilde{\mathbf{y}}_{tf}\}_{f=1}^F, \mathbf{e}_t\}$. Here, $\tilde{\mathbf{y}}_{tf} \in \mathbb{C}^C$ denote the length-normalized multi-channel STFT features of the meeting with time frame index t , frequency bin index f , and the frame-level speaker embeddings \mathbf{e}_t are obtained with a pre-trained speaker embedding extractor, such as [18]. The first captures spatial, and the second spectral information in the joint model

$$p(\mathcal{O}_t) = \prod_f \sum_k \pi_{kt} p^{\text{VMF}}(\mathbf{e}_t | z_{ktf} = 1) p^{\text{cACG}}(\tilde{\mathbf{y}}_{tf} | z_{ktf} = 1), \quad (1)$$

respectively. π_{kt} is the time-dependent prior probability of each speaker in the meeting as introduced in [19]. For the integrated model, a von-Mises-Fisher Mixture Model (vMFMM) [20] and a cACGMM [19] with respective component distributions $p^{\text{VMF}}(\cdot)$ [21] and $p^{\text{cACG}}(\cdot)$ [22] are combined to perform diarization and separation jointly, by estimating the latent variables z_{ktf} of each speaker k with the EM algorithm. For the remainder of this work, the latent variables are denoted without the condition of Eq. (1) due to space constraints. The vMF distribution is specified by an average orientation μ and the concentration parameter κ , which can be interpreted as the average speaker embedding and embedding uncertainty of a speaker in a meeting, while the cACG distribution is determined by the frequency-dependent spatial covariance matrix \mathbf{B}_f , which models the spatial cues of a location with active speech.

The posterior probabilities $p(z_{ktf} | \mathcal{O}_t)$ then serve as mask estimates for each tf-bin and speaker k and are used to reconstruct the individual utterances of the recording through beamforming. The graphical model of this tightly integrated model, i.e., a model using joint latent variables, is visualized in Fig. 1.

While the spatial mixture model is able to assign each tf-bin to a mixture component in this setup, the spectral mixture model attributes all frequency bins $f \in \{1, \dots, F\}$ of a given time frame t to the same class. This automatically introduces a mismatch in time frames, where a speaker is not active in all frequencies. Further note that because a mixture component represents a speaker in the spectral model and a location in the spatial model, the tight coupling of the two models via the shared latent variable induces the assumption that there is a one-to-one mapping between speaker and location.

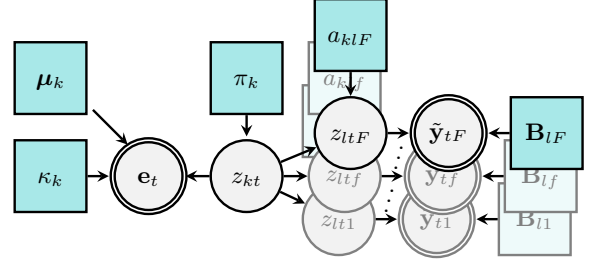


Fig. 2. Graphical model of the loose coupling. The latent variable z_{kt} of the spectral model serves as prior for the latent variables z_{ltf} of the spatial models, which are fitted per frequency $f \in \{1, \dots, F\}$.

This prevents the modeling of moving speakers, because if a speaker speaks from different positions, multiple spatial components need to be mapped to the same spectral mixture component. Therefore, the tight coupling is by design incapable of tracking position changes.

3. LOOSE COUPLING OF MIXTURE MODELS

To address both systematic issues of the tight integration, we propose to replace the above tight by a loose coupling of the vMFMM and cACGMM. This is done by reformulating the integration with one latent variable z_{kt}^{vM} for the spectral and another, z_{ltf}^{cAC} , for the spatial mixture model, respectively.

These two latent variables are assumed to be conditionally dependent with

$$p(z_{ltf}^{\text{cAC}} | z_{kt}^{\text{vM}}) = a_{klf} \text{ with } \sum_l a_{klf} = 1, \quad (2)$$

formulating the spectral, time-dependent affiliation z_{kt}^{vM} as prior for the spatial, time-frequency dependent affiliation z_{ltf}^{cAC} . This allows the number of spectral VMF mixture components K to be different from the number of spatial cACG mixture components L . The likelihood of the observed data is then given by

$$\begin{aligned} p(\mathcal{O}_t) &= \sum_{k, l_1 \dots l_F} \pi_k p(\mathbf{e}_t | z_{kt}^{\text{vM}}) \prod_f a_{klf} p(\tilde{\mathbf{y}}_{tf} | z_{ltf}^{\text{cAC}}) \\ &= \sum_k \pi_k p(\mathbf{e}_t | z_{kt}^{\text{vM}}) \prod_f \sum_l a_{klf} p(\tilde{\mathbf{y}}_{tf} | z_{ltf}^{\text{cAC}}), \end{aligned} \quad (3)$$

where the coupling factors a_{klf} can be viewed as the probability of a speaker being active from location l given that speaker k is active, and the prior π_k of the spectral variables describes the probability of speaker k being active. The graphical model is visualized in Fig. 2.

In this way, the spectral model determines whether a speaker is active for a given time frame, while the spatial model can still portray inactivity for certain frequency bins at this time frame. At the same time, the loose coupling also allows for multiple spatial mixture components to correspond to the same speaker. Therefore, the model allows for a speaker being active from multiple locations over the course of the processed segments. Multiple spatial mixture components can also represent the same speaker by capturing strong reflections from walls, which makes the same speaker appear active from different positions.

In order to fit this model to the observations \mathcal{O} , the EM algorithm is employed. As in [17], the M-step to estimate the distribution parameters $\Theta = \{\mu_k, \kappa_k, \pi_k, \mathbf{B}_{lf} \ \forall k, l, f\}$ remains unchanged compared to an individual vMFMM or cACGMM, with the difference being that the respective latent variables z_{kt}^{vM} and z_{ltf}^{cAC} are used.

For the E-step, the individual latent variables can be estimated by first obtaining the joint latent posterior

$$\delta_{kltf} = p(z_{kt}^{\text{vM}}, z_{ltf}^{\text{cAC}} | \mathcal{O}_t, \Theta) = \frac{\pi_k p(\mathbf{e}_t | z_{kt}^{\text{vM}}) \alpha_{kltf} p(\tilde{\mathbf{y}}_{tf} | z_{ltf}^{\text{cAC}})}{p(\mathcal{O}_t)} \left(\prod_{f' \neq f} \sum_l \alpha_{kltf'} p(\tilde{\mathbf{y}}_{tf'} | z_{ltf'}^{\text{cAC}}) \right), \quad (4)$$

from which the estimates of the individual posteriors

$$p(z_{kt}^{\text{vM}} | \mathcal{O}_t) = \frac{1}{F} \sum_l \sum_f \delta_{kltf}, \quad p(z_{ltf}^{\text{cAC}} | \mathcal{O}_t) = \sum_k \delta_{kltf} \quad (5)$$

can be obtained via marginalization. The newly introduced coupling weights are estimated in the M-step by

$$\alpha_{kltf} = \frac{\sum_t \delta_{kltf}}{\sum_t \sum_l \delta_{kltf}}. \quad (6)$$

3.1. Mask estimation for loosely coupled models

Contrary to the tight integration of Section 2, the affiliations of the loosely coupled model cannot be directly interpreted as mask estimates for each speaker in the processed recording. The mixture model only contains location-specific affiliations z_{ltf}^{cAC} and speaker-specific diarization affiliations z_{kt}^{vM} . For speech extraction, speaker-specific mask estimates m_{ktf} are required in order to apply them for mask-based beamforming. Since only the spatial model, which is dependent on l , depicts frequency-dependent information, marginalization over the locations of the joint posterior δ_{kltf} results in a constant solution over all frequencies. This is undesirable for the extraction process since it impairs the performance, especially in regions of multiple active speakers and strong background noise.

Instead, to make the estimation more reliable, we introduce heuristics for the weight calculation and the modification of the joint posterior. First, the probability that a speaker is active, given that the location is active for a single frequency f

$$\beta_{klf} = p(z_{kt}^{\text{vM}} | z_{ltf}^{\text{cAC}}, \mathcal{O}_t) \quad (7)$$

is estimated complementary to the coupling factors α_{kltf} . Then, these values are used as a weighting factor for the joint posterior to obtain frequency-selective masks. β_{klf} is estimated by first removing the location corresponding to noise from the joint posterior δ_{kltf} . This location is identified as the one carrying the highest overall activity, as was done in [14], since speech sources carry only sparse activity. Then, similar to Eq. (6), the reduced posterior $\tilde{\delta}_{kltf}$ without noise component is used to estimate

$$\beta_{klf} = \frac{\sum_t \tilde{\delta}_{kltf}}{\sum_t \sum_k \tilde{\delta}_{kltf}} \quad (8)$$

directly from the joint posterior. To account for noise contributions in the remaining location components, β_{klf} is then thresholded at

$$\tilde{\beta}_{klf} = \begin{cases} \beta_{klf} & \text{if } \beta_{klf} \geq \tau_{\text{th}} \\ 0 & \text{else} \end{cases} \quad (9)$$

with the threshold $\tau_{\text{th}} = 0.55$ to only consider the relevant positions and not reflections or noise interference. Finally, the mask estimates

$$m_{ktf} = \sum_l \tilde{\beta}_{klf} \tilde{\delta}_{kltf}. \quad (10)$$

are obtained by multiplying the mapping of location to speaker with the joint posterior before marginalization of the locations.

4. EVALUATION

We evaluate the model using the LibriCSS database [23], which consists of re-recorded, simulated meetings of 8 stationary speakers containing 0 % to 40 % overlapping speech (OS – OV40). Here, the performance is evaluated both on the LibriCSS segments, a predefined split of the LibriCSS meetings at silence with an average segment duration of 50 s, and a concatenated version of the LibriCSS segments. For this version, two segments of the same session are concatenated such that each segment is used only once and the number of speakers common to both segments is maximized¹, resulting in an average segment duration of 75 s.

In addition, an evaluation set with speaker position changes is simulated for the concatenated segments by rotating all non-center microphone channels by two positions in the latter segment, effectively causing each speaker to move by 120°. For this setup, which we call speaker relocation, on average, 3.2 active speakers are common to both segments.

For the initialization of the loose coupling, the joint posterior δ_{kltf} is initialized via an individual spectral and spatial initialization. For the spectral initialization, a fusion-based scheme as proposed in [17] is employed. First, an energy-based Voice Activity Detection (VAD) using minimum statistics is applied to run a k-Means clustering using $2K$ classes on the embeddings corresponding to speech. Then, a vMFMM is fitted to the data, where the mixture components with the highest similarity are fused until K clusters remain. These activity estimates for the speakers are then extended across the speech pauses detected by the VAD, obtaining z_{kt}^0 . Alternatively, we also investigate using the diarization target as oracle initialization as a reference. For the initialization of the spatial model, the clustering-based approach from [14] is used. Following that, a cACGMM is fitted to the data for 30 iterations to stabilize the spatial initialization z_{ltf}^0 . We assume the number of speakers N in a segment is known and choose $K = N$ spectral components and $L = 2N + 1$ spatial positions w.l.o.g., providing two positions for each speaker as well as an additional noise class. The initial estimates of the spectral and spatial initialization are finally combined into the initial $\delta_{kltf}^0 = z_{kt}^0 z_{ltf}^0$. Following that, the model is started with an M-step to obtain the parameters Θ .

We compare the loose coupling with a cACGMM from [14] and the tight integration from [17] as baselines, where each model is fitted for 100 EM iterations to ensure convergence. The detected activity is first smoothed, and duplicates of speakers are removed, which are identified by comparing the intersection of their activity patterns and their prototypical speaker representations μ .

Then, a masked-based MVDR beamformer [24] is applied, and the utterances are transcribed with a Conformer-based ASR model from the Nemo toolkit [25, 26]. The performance is compared in terms of the concatenated minimum-permutation Word Error Rate (cpWER) [27] calculated with the MeetEval toolkit [28].

4.1. Evaluation in the presence of speaker position changes

First, the performance on the concatenated LibriCSS segments without microphone channel rotation is compared against the relocation setup with channel rotation to directly assess the influence of position changes. The results are shown in Table 1.

For the static scenario, the loose coupling consistently shows an improvement over the tight integration, both for an oracle diarization and a non-oracle initialization of the spectral model. For an oracle initialization, the loose coupling shows an improvement of 1.1 %

¹<https://zenodo.org/records/17121135>

Table 1. cpWER of the tight integration and loosely coupled system on the concatenated LibriCSS segments for the *static* (left) and the *speaker relocation* (right) scenario. “orc. init” denotes an initialization with the oracle diarization.

System	orc. init	0S	0L	OV10	OV20	OV30	OV40	avg.
cACGMM	✓	4.2 / 19.7	4.1 / 23.0	3.5 / 22.0	4.6 / 24.2	7.9 / 28.3	6.4 / 29.7	5.3 / 24.8
tight int.	✓	4.2 / 17.2	4.4 / 21.9	4.2 / 19.4	5.1 / 23.4	5.8 / 25.9	5.9 / 27.8	5.0 / 22.9
loose coupling	✓	5.0 / 5.0	3.5 / 5.0	2.7 / 5.0	3.4 / 6.8	4.3 / 11.1	4.1 / 12.7	3.9 / 8.0
tight int.	-	6.9 / 22.3	4.7 / 34.3	6.9 / 25.3	7.8 / 25.9	9.1 / 28.2	9.4 / 30.1	7.7 / 27.5
loose coupling	-	6.9 / 9.3	5.3 / 8.4	4.0 / 9.2	5.8 / 12.9	6.9 / 15.2	7.0 / 19.4	6.0 / 12.9

Table 2. cpWER of the tight integration and loosely coupled system on individual LibriCSS segments. “orc.” denotes an initialization with the oracle diarization.

System	orc.	0S	0L	OV10	OV20	OV30	OV40	avg.
tight int.	✓	4.8	3.8	3.1	4.2	5.0	4.9	4.3
loose coup.	✓	4.7	2.9	3.4	3.7	4.3	4.6	4.0
tight int.	-	4.3	5.9	3.9	4.9	6.5	6.8	5.4
loose coup.	-	5.8	4.5	5.1	4.9	6.7	7.1	5.8

absolute in terms of cpWER, while this improvement increases to 1.7 % for a non-oracle initialization. However, both the tight integration and the loose coupling increasingly lose performance for higher overlap subsets with a non-oracle initialization. This effect is likely to come from the higher complexity of capturing all speakers active in a segment, since speakers with little or no single-speaker activity become more likely to appear for higher overlaps.

When comparing the static results (left) with the *relocation* subset (right) in Table 1, the main advantage of the loose coupling becomes apparent. Here, the tight integration fails to stabilize the system in the case of moving speakers. Even for an oracle initialization, the model is incapable of maintaining the diarization estimate, resulting in an increase in cpWER from 5.0 % to 22.9 %. This is almost as bad as when solely using a cACGMM, which by design is a fully spatial model and incapable of tracking any position changes. Compared to that, the loose coupling outperforms the tight integration by 14.9 % and 14.6 % absolute for an oracle and non-oracle initialization, respectively. With corresponding average cpWERs of 8.0 % and 12.9 %, this still indicates a large performance loss compared to the static scenario, even if not as severe as for the tight integration. However, when referring to the individual overlap subsets, it turns out that the performance loss of the loosely coupled model predominantly occurs for the high-overlap subsets.

This is similar to the results of the frame-level speaker embeddings of [18], where a Diarization Error Rate (DER) of more than 30 % occurs when scoring only overlapping speech. This implies that the embedding quality is significantly lower for regions of overlapping speech. Therefore, we conjecture that the worse embedding quality under overlapping speech, jointly with the increased complexity of moving speakers, leads to higher amounts of missed speakers and speaker swaps, which negatively impact the WER. Still, the model proves able to stabilize the performance in case of changing speaker positions, especially for low overlap ratios.

4.2. Performance in a stationary environment

To directly assess the loose coupling’s performance compared to the tight integration from [17], the performance is also compared on the individual LibriCSS segments. Table 2 shows this comparison. Similar to the concatenated LibriCSS segments, the loose coupling is

able to show an improvement upon the tight integration for oracle initialization, which is likely to come from the frequency selectivity and higher flexibility in terms of mapping multiple locations to the same speaker components.

Contrary to the concatenated setup, for a non-oracle initialization, the loose model incurs performance losses compared to the tight integration, resulting in a performance drop from 5.4 % to 5.8 % cpWER. Again, the performance loss is more prominent for overlapping speech. Since the loose coupling puts a high reliance on the spectral features by using them as a prior for the spatial model, in cases where the frame-wise embeddings or the spectral initialization become unreliable, the spatial model can not as easily compensate for this information as for the tight integration. Further, the quality of the spectral initialization becomes more important and a limiting factor of the performance which matches the findings from Section 4.1. However, by using a better spectral initialization, as shown for the use of oracle information, the model can be guided to a better solution during the fitting process.

As the loose coupling needs to estimate the coupling weights during the fitting process of the model, it benefits more from a higher amount of observations which can also help for a better spectral initialization. Therefore, the loose coupling still shows an improvement upon the tight integration for longer segments as discussed in Section 4.1, even in a static scenario.

5. CONCLUSION

In this work, we proposed a statistical dependence for mapping spatial and spectral mixture models in the context of meeting processing and introduced a way to obtain mask estimates from this loosely coupled model. We were able to demonstrate that the loosely coupled system outperforms a tight integration of both models in the case of an oracle diarization. In case of longer segments, as is the case for a concatenation of two LibriCSS segments, the loose coupling model also outperforms a tight integration for a non-oracle initialization. In addition, the loosely coupled model proves able to handle speakers being active from multiple positions, whereas the tight integration is unable to resolve mismatching spatial and spectral cues.

Currently, the loosely coupled model still suffers from performance degradation as the degree of overlapping speech increases. In addition, it seemingly requires more observations to perform a stable fitting process compared to the tight integration. Therefore, future work will aim at incorporating spectral observations with higher stability, especially for overlapping speech, and the application of the loose coupling to recordings with real speaker movements to increase the model robustness and assess the performance for speaker trajectories.

6. ACKNOWLEDGMENTS

Computational resources were provided by BMBF/NHR/PC2

7. REFERENCES

- [1] J. M. Pardo, X. Anguera, and C. Wooters, “Speaker diarization for multi-microphone meetings using only between-channel differences,” in *International Workshop on Machine Learning for Multimodal Interaction*. Springer, 2006, pp. 257–264.
- [2] S. Araki, M. Fujimoto, K. Ishizuka, et al., “A DOA based speaker diarization system for real meetings,” in *Hands-Free Speech Communication and Microphone Arrays*. IEEE, 2008, pp. 29–32.
- [3] T. Hager, S. Araki, K. Ishizuka, et al., “Handling speaker position changes in a meeting diarization system by combining DOA clustering and speaker identification,” in *Proc. IEEE IWAENC*, 2008, vol. 106.
- [4] D. Snyder, D. Garcia-Romero, G. Sell, A. McCree, D. Povey, and S. Khudanpur, “Speaker recognition for multi-speaker conversations using x-vectors,” in *Proc. ICASSP*, 2019, pp. 5796–5800.
- [5] Y. Fujita, N. Kanda, S. Horiguchi, K. Nagamatsu, and S. Watanabe, “End-to-end neural speaker diarization with permutation-free objectives,” in *Proc. Interspeech*, 2019, pp. 4300–4304.
- [6] S. Horiguchi, Y. Fujita, S. Watanabe, Y. Xue, and K. Nagamatsu, “End-to-end speaker diarization for an unknown number of speakers with encoder-decoder based attractors,” in *Proc. Interspeech*, 2020, pp. 269–273.
- [7] K. Kinoshita, M. Delcroix, and N. Tawara, “Integrating end-to-end neural and clustering-based diarization: Getting the best of both worlds,” in *Proc. ICASSP*. IEEE, 2021, pp. 7198–7202.
- [8] A. Plaquet and H. Bredin, “Powerset multi-class cross entropy loss for neural speaker diarization,” in *Proc. Interspeech*, 2023.
- [9] J. Han, F. Landini, J. Rohdin, A. Silnova, M. Diez, and L. Burget, “Leveraging self-supervised learning for speaker diarization,” in *Proc. ICASSP*, 2025.
- [10] S. Horiguchi, Y. Takashima, P. García, S. Watanabe, and Y. Kawaguchi, “Multi-channel end-to-end neural diarization with distributed microphones,” in *Proc. ICASSP*, 2022, pp. 7332–7336.
- [11] N. Zheng, N. Li, J. Yu, C. Weng, D. Su, X. Liu, and H. Meng, “Multi-channel speaker diarization using spatial features for meetings,” in *Proc. ICASSP*, 2022, pp. 7337–7341.
- [12] R. Wang, S. Niu, G. Yang, J. Du, S. Qian, T. Gao, and J. Pan, “Incorporating spatial cues in modular speaker diarization for multi-channel multi-party meetings,” *arXiv preprint arXiv:2409.16803*, 2024.
- [13] R. Haeb-Umbach, T. Nakatani, M. Delcroix, C. Boeddeker, and T. Ochiai, “Microphone array signal processing and deep learning for speech enhancement: Combining model-based and data-driven approaches to parameter estimation and filtering,” *IEEE Signal Processing Magazine*, vol. 41, no. 6, pp. 12–23, 2024.
- [14] C. Boeddeker, T. Cord-Landwehr, T. von Neumann, and R. Haeb-Umbach, “An initialization scheme for meeting separation with spatial mixture models,” in *Proc. Interspeech*, 2022.
- [15] C. Boeddeker, J. Heitkaemper, J. Schmalenstroer, L. Drude, J. Heymann, and R. Haeb-Umbach, “Front-end processing for the CHiME-5 dinner party scenario,” in *Proc. CHiME*, 2018, pp. 35–40.
- [16] H. Taherian and D. Wang, “Multi-channel conversational speaker separation via neural diarization,” *IEEE Trans. Signal Process.*, vol. 32, pp. 2467–2476, 2024.
- [17] T. Cord-Landwehr, C. Boeddeker, and R. Haeb-Umbach, “Simultaneous diarization and separation of meetings through the integration of statistical mixture models,” in *Proc. ICASSP*. IEEE, 2025, pp. 1–5.
- [18] T. Cord-Landwehr, C. Boeddeker, C. Zorilă, R. Doddipatla, and R. Haeb-Umbach, “Geodesic interpolation of frame-wise speaker embeddings for the diarization of meeting scenarios,” in *Proc. ICASSP*. IEEE, 2024, pp. 11886–11890.
- [19] N. Ito, S. Araki, and T. Nakatani, “Complex angular central gaussian mixture model for directional statistics in mask-based microphone array signal processing,” in *Proc. EUSIPCO*, 2016, pp. 1153–1157.
- [20] A. Banerjee, I. S. Dhillon, J. Ghosh, and S. Sra, “Clustering on the unit hypersphere using von mises-fisher distributions,” *Journal of Machine Learning Research*, vol. 6, no. 46, pp. 1345–1382, 2005.
- [21] R. A. Fisher, “Dispersion on a sphere,” *Proceedings of the Royal Society of London. Series A. Mathematical and Physical Sciences*, vol. 217, no. 1130, pp. 295–305, 1953.
- [22] D. E. Tyler, “Statistical analysis for the angular central gaussian distribution on the sphere,” *Biometrika*, vol. 74, no. 3, pp. 579–589, 1987.
- [23] Z. Chen, T. Yoshioka, L. Lu, T. Zhou, Z. Meng, Y. Luo, J. Wu, X. Xiao, and J. Li, “Continuous speech separation: Dataset and analysis,” in *Proc. ICASSP*, 2020, pp. 7284–7288.
- [24] M. Souden, J. Benesty, and S. Affes, “On optimal frequency-domain multichannel linear filtering for noise reduction,” *IEEE Trans. Signal Process.*, vol. 18, no. 2, pp. 260–276, 2009.
- [25] D. Rekesh, N. R. Koluguri, S. Kriman, S. Majumdar, V. Noroozi, H. Huang, O. Hrinchuk, K. Puvvada, A. Kumar, J. Balam, et al., “Fast conformer with linearly scalable attention for efficient speech recognition,” in *Proc. ASRU*, 2023, pp. 1–8.
- [26] O. Kuchaiev, “Nemo pretrained model, nvidia/stt_en.conformer.ctc.large,” 2022.
- [27] S. Watanabe, M. Mandel, J. Barker, E. Vincent, A. Arora, X. Chang, S. Khudanpur, V. Manohar, D. Povey, D. Raj, D. Snyder, A. S. Subramanian, J. Trmal, B. B. Yair, C. Boeddeker, Z. Ni, Y. Fujita, S. Horiguchi, N. Kanda, T. Yoshioka, and N. Ryant, “Chime-6 challenge: Tackling multispeaker speech recognition for unsegmented recordings,” in *Proc. CHiME*, 2020, pp. 1–7.
- [28] T. von Neumann, C. Boeddeker, M. Delcroix, and R. Haeb-Umbach, “MeetEval: A toolkit for computation of word error rates for meeting transcription systems,” in *Proc. CHiME*, 2023, pp. 27–32.